Upgrading to IGBT transistors traction converters with GTO thyristors

João Formiga, J. Fernando Silva
Instituto Superior Técnico, UL, Lisbon
E-mail:joao.formiga@ist.utl.pt

***Abstract* — The present work aims to study the upgrading of electric rail traction converters. Each traction converter comprises a two-quadrant reversible voltage converter, being the M1 and M2 Modules the arms of the converter. The need to perform this update is related to the fact that the GTO's used in these Modules are obsolete and approaching the end of its lifetime. The proposed solution consists in replacing the GTO modules and their gate units, with a new technology of IGBT transistors (Press-pack IGBT) and their gate units. These technology features an IGBT packaging format compatible with existing physical structure of either the converter and the existing GTO's.**

***Index Terms* — traction converter, two-quadrant converter, GTO, IGBT, gate units.**

I. Introduction

The electric rail traction converter in study, consists in a three phase induction motors fed by GTO thyristor power converters. Each power converter comprises a DC chopper (two-quadrant converter), being the M1 and M2 modules the arms of the converter. These modules are the elements of analysis in this work. The converter contains also an intermediate energy storage circuit (which consists in an inductance that smooths the current) and a thyristor current source inverter that generates a three-phase currents system to fed the motors.

The two-quadrant chopper is a reversible voltage buck-converter controlled with pulse modulation (PWM – "Pulse-Width Modulation"), allowing the passage of continuous drive line voltage (for example 750 V +20%, -30 %) to the values of the chopper output voltage (approximately 600 V in motoring). These processes are performed by microprocessors embedded in the traction control system modules.

Thus, in the traction mode, the DC chopper supplies a DC current – using the PWM – to the intermediate circuit, which makes the cyclic distribution of the current to the motors. In braking mode, prevails the regenerative braking, increasing the line voltage. When the maximum allowable value of the line is reached, the chopper braking system comes into operation, dissipating the excess energy.

The M1 and M2 modules contains, each one, 2 parallel GTO's thyristors (supporting forward voltages of 4500 V and capable of interrupt currents of 3000 A). Each GTO has 125 Hz of switching frequency, enabling the module a full operating frequency of 250 Hz.

The GTO's have been the most used semiconductor in high voltage DC choppers for the past 30 years. As in many converters, the GTO's in this electric rail traction converter are getting obsolete. Therefore, in this work, it is studied the possibility of the replacement of this semiconductors by "Press-Pack IGBT's" and analyzed the impact that this change has in the efficiency of the converter.

II. M1/M2 Modules

Figure 1 illustrates the power converter in study. The converter has a two-quadrant chopper – M1 and M2 modules –, an intermediate circuit represented by the L1 inductance and a phase-sequence inverter with 6 thyristors and corresponding commutation capacitors, that delivers the current to the motors generating a three-phase system.

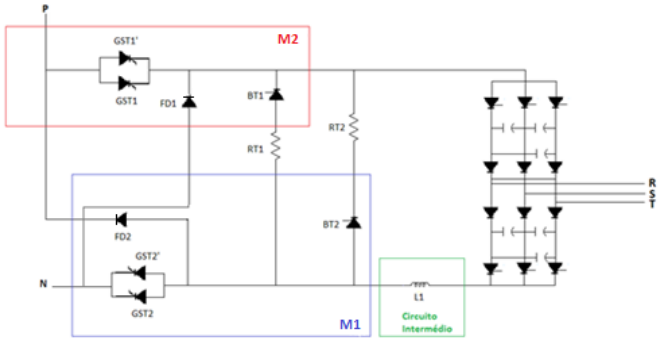

Figure 1 - Simplified traction converter of the electric rail traction converter in study.

As indicated in figure 1, the M1/M2 Modules consists in two GTO thyristors in parallel, a freewheeling diode and a conventional thyristor. The fact that the two GTO's are in parallel allows the doubling of the converter frequency of operation. Each GTO operates at 125 Hz, giving an equivalent

of 250 Hz commutation frequency.

The M1 and M2 modules, together form the two-quadrant voltage reversible converter.

A. *M1 Module*

Figure 2 illustrates the configuration of the M1 Module.

To take advantage of the GTO's parallel, anti-phase control signals are used to each one of the GTO's. Therefore, the GTO's are, alternately, in the on-state, supporting the entire current.

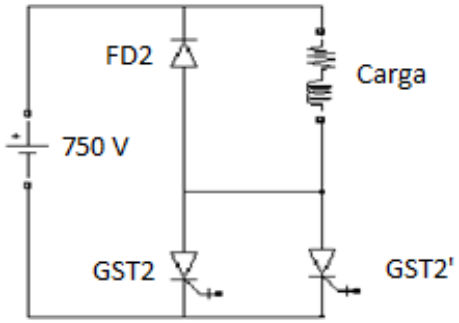

Figure 2 - M1 Module.

There are two states that the module can assume. In the first state, one of the GTO's (GST2) is on and the freewheeling diode (FD2) and the other GTO (GST2') are off. In the second state FD2 is on and the GTO's are off. These states are illustrated in figure 3.

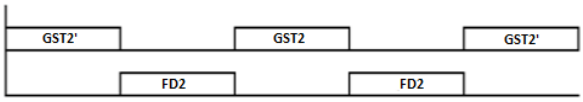

Figure 3 - Driving mode of the M1 Module.

B. *M2 Module*

The constitution of this module is the same as the M1, being the representation symmetric to Figure 2.

The driving mode of the M2 module is represented in figure 4.

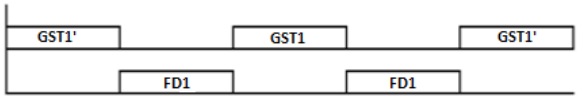

Figure 4 - Driving mode of the M2 Module.

C. *Determination of the M1/M2 parameters*

The duty-cycle of each GTO is given by [1]:

$$\delta = \frac{V_0}{U} \tag{1}$$

Therefore, with $V_0 = 600\ V$ and $U = 750\ V$ we obtain, for each GTO, $\delta = 0{,}4$.

Knowing that $I_0 = 780\ A$, we obtain for the load resistance:

$$R_0 = \frac{V_0}{I_0} \approx 0{,}77\ \Omega \tag{2}$$

The inductance load is given by [1]:

$$L_i = \frac{U(1-\delta)\delta T}{\Delta i_{Li}} = \frac{U(1-\delta)\delta\frac{1}{f}}{\Delta i_{Li}} \tag{3}$$

With $\Delta i_{Li} = 0{,}1 \times I_0$ and $f = 250\ Hz$, results $L_i \approx 6{,}15\ mH$.

In figure 3, it is represented the voltage and current across the GTO's, the freewheeling diode and the load, during the commutations that lead the semiconductors to the two states referred above.

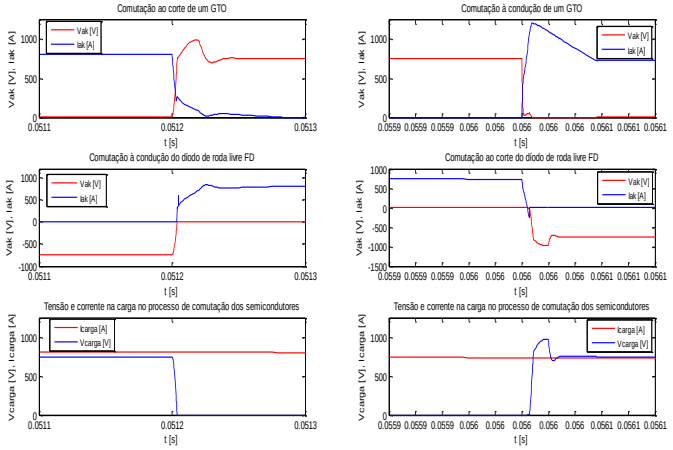

Figure 5 - States of the M1/M2 Modules

The output power of the Modules is:

$$P_0 = V_0 I_0 = 468\ kW \tag{4}$$

The average current to be driven by the GTO's is determined attending the following expression:

$$I_{GTO_{av}} = \frac{I_o}{2}\,\delta = 312\ A \tag{5}$$

On the other hand, the RMS current is given by:

$$I_{GTO_{RMS}} = \frac{I_o}{2}\sqrt{\delta} \approx 342{,}83\ A \tag{6}$$

In the freewheeling diode, the average and RMS currents are:

$$I_{D_{av}} = (1 - \delta)I_o = 156\ A \tag{7}$$

$$I_{D_{RMS}} = I_o\sqrt{(1-\delta)} \approx 348{,}83\ A \tag{8}$$

The maximum voltages to be supported by the GTO's and freewheeling diode are calculated by:

$$V_{AKmax} = 750 + 20\% = 900V \tag{9}$$

$$V_{RRM} = 750 + 20\% = 900V \tag{10}$$

D. *Freewheeling Diode*

The freewheeling diode used in the modules is a fast soft recovery diode produced by *Siemens* (SSi model). In diodes a phenomenon, designated by reverse recovery, occurs which results from the attempt of abruptly change the diode polarization to the reverse zone. In the reverse recovery phenomenon, an important reverse recovery current appears due to the high value of the reverse voltage across the diode during the off-state commutation.

Due to the fact that the *Matlab/Simulink* modules are unable to represent the reverse recovery occurrence, it was created a MOSFET based model with that purpose. This model is illustrated in figure 6.

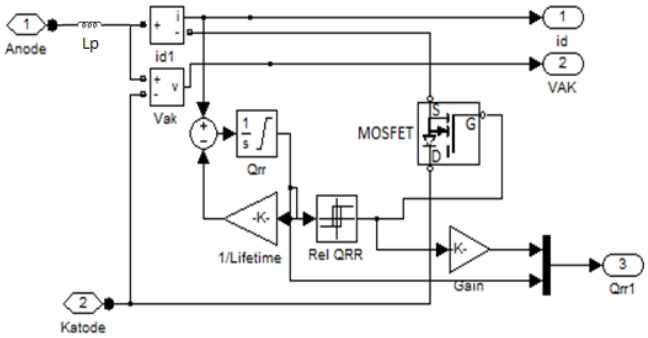

Figure 6 - Reverse recovery diode model.

The model uses a MOSFET with an intrinsic antiparallel diode, so that the device can carry current in both ways when the voltage becomes negative. The model also contains a charge controlled feedback loop that controls the gate of the MOSFET. In the feedback loop it is used an integrator to obtain the charge:

$$\int \left(i - \frac{Q}{t_{rr}}\right) dt = Q_{RR} \qquad (11)$$

The integrator used in figure 6 has Q_{RR} as the maximum saturation limit, to assume that value whenever the result of the integral is greater or equal to Q_{RR}.

Figure 7 shows the v_{AK} and i_{AK} waveforms obtained with the model illustrated above, during turn-off commutation, under the M1/M2 operating conditions.

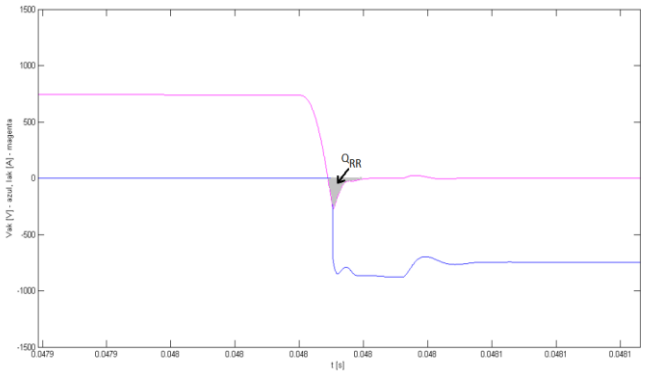

Figure 7 - Dynamic behavior of the freewheeling diode at turn-off

Analyzing the figure 7 and observing the area that the reverse recovery charge Q_{RR} holds, it is demonstrated that the model reproduces the behavior of a fast soft recovery diode. The reverse recovery charge corresponds to the total area bounded by the reverse recovery current whose maximum is $I_{RR} = 200$ A.

III. GTO (GATE TURN-OFF THYRISTOR)

The GTO used in the M1 and M2 modules, is a bipolar semiconductor device with thyristor distributed cathode structures, capable of blocking high voltages (several hundred volts) in the off-state and able to drive several hundred amperes currents in the on-state.

This device switches to the on-state by applying a current pulse at the gate and maintains this state using a current gate value lower than the necessary pulse to switch-on.

The GTO's in the M1/M2 Modules are silicon semiconductors with a case similar to a wafer or a disc hockey and are manufactured by *Toshiba* (SG3 model).

In figure 8 is illustrated the scheme in *Simulink* of the parallel of the GTO's.

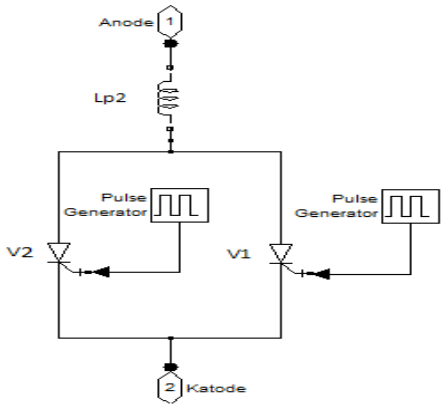

Figure 8 - Parallel of the GTO's in M1 Module.

The gate drive of the GTO's is performed by a pulse generator that only indicates the on-state period of each GTO and the phase shift between them. The pulse generator only works with amplitudes of 0 and 1, with the aim of producing simple command turn-on and turn-off commutations.

The L_{p2} inductance concentrates all the parasitic inductances in one coil – considering that they are about 10 cm of cable in the converter circuit –, accounting for nearly 0,1 µH.

The inductance makes the turn-off waveforms closer from the real waveforms, since the introduction of L_{p2} allows the rising of the voltage v_{AK} before i_{AK} starts to drop.

A. *Losses determination*

The on-state losses of each GTO can be determined by the following expression:

$$P_{dGTO} = V_D\, i_{AKDC} + r_D I^2_{AKRMS} \qquad (12)$$

Considering $V_D = 1{,}7\,V$ and $r_D = 1{,}2\,m\Omega$ (according to datasheet), the conducting losses are $P_{dGTO} \approx 671{,}444$ W.

The switching losses are given by:

$$P_{sGTO} = V_{AK}\, I_{AK}\, \frac{t_r + t_f}{6T} \quad (13)$$

With $t_r = 7\mu s$ and $t_f = 3\mu s$ (according to datasheet), results $P_{sGTO} \approx 121{,}88$ W.

The additional losses in the turn-off commutation, associated with the tail current, can be determined by:

$$P_{sOFFGTO} = V_{AK}\, I_{tail}\, \frac{t_{tail}}{2T} \quad (14)$$

With $I_{tail} = 81$ A obtained by simulation (using the model explained in Section V), results $P_{sOFFGTO} \approx 303{,}75$ W.

B. GTO Gate unit

The responsible equipment for controlling the GTO's in the M1/M2 modules are the Central Control Systems (SCC and SCT) and the A10 gate module. SCC and SCT undertake the processing of all information in the electric rail train converter, while the A10 gate unit is the module responsible to control the commands given to the GTO's.

The A10 module is composed by A1, A2 and A3 units. The A1 unit is responsible for the connection between SCT and the A10 module, receiving the driving signals that indicate the GTO's to be on or off. The A2 and A3 units feed the demodulating unit by mean of a rectifier coupled to a transformer.

Figure 9 – Example of the A10 gate unit.

IV. PRESS-PACK IGBT

The GTO's substituted under analyses in this work are the new IGBT technology, called Press-pack IGBT.

A. Electromechanical characteristics of Press-Pack IGBT's

The Press-pack IGBT's study in this work are produced by *Westcode Semiconductors*. These devices are capable of withstanding high voltages (kV) and currents, and their configuration is achieved by packaging many small chips (special produced) in similar structures to the so-called wafers. The chips and the base that hold them are undoubtedly the key of Press-Pack IGBT's electromechanical performance.

It is known that the long-term reliability of the module IGBT, in some applications, is still questionable. To overcome the known failure modes, a completely bond free, pressure contact IGBT package has been developed, along with the specially designed chips, which have been optimized for operation under pressure contact. [13]

Figure 11 a) shows the typical design used in a wire bonded construction with the gate contact at the center and eight emitter cell groups with centrally located bonding contacts to take the emitter bond wires. In figure 11 b), it is illustrated the new design that allows maximum use of the remainder of the chip for a flat emitter pressure contact.

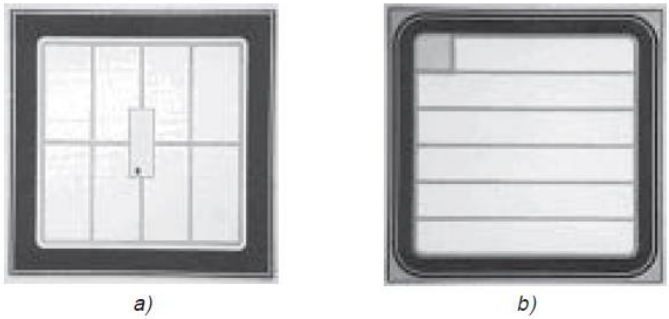

Figure 10 - a) Center gate; b) Corner gate [13].

The basic mechanical construction for a single IGBT chip is shown in figure 11. In figure 11 a) is illustrated the exploded view of the chip locator and in figure 11 b) is the compressed view of chip locator.

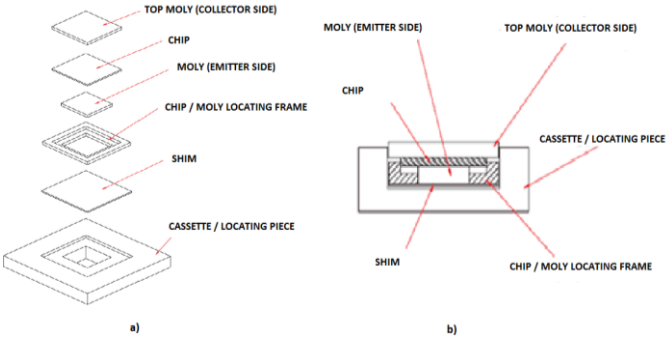

Figure 11 - a) Exploded view of chip locator; b) Compressed view of chip locator. [13]

Each chip is mounted into an integral carrier ("Cassette/Locating Piece") that combines the required number of IGBT and diode chips into a single unit for pre-testing prior to encapsulation [13]. However, in this work only IGBT's are used in the chips locator, because the purpose of the diodes is to allow the set "IGBT+diode" driving current in both ways, which is not necessary given the inclusion of the freewheeling diodes in the M1/M2 Modules.

The *Westcode* Press-Pack IGBT, contrary to other manufactures, has no bond wire to connect the gates. The connection is made by a planar contact system. The concept of this assembly is illustrated in figure 12.

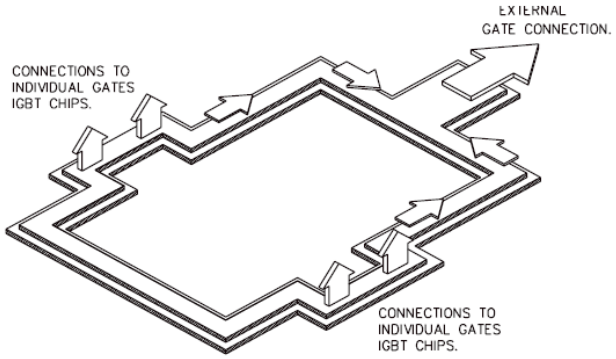

Figure 12 - Planar gate track. [13]

A spring loaded contact pin connects the gate of the chip to the planar distribution system, which in turn connects to the external gate terminal [13].

Figure 13 shows the connection between the planar gate distribution system and the individual gate chips (made through the corner of the gates).

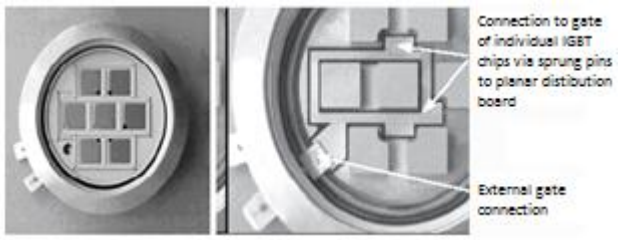

Figure 13 - Planar gate distribution system. [15]

This kind of technology, where the devices are housed in conventional hermetic ceramic packages, offers the possibility of integrating the Press-Pack IGBT in the M1/M2 Modules with an exceptional electromechanical performance.

In this paper we study the integration of 3 different Press-Pack IGBT. The 3 models are capable of support up to 4,5 kV with currents rated up to 1200 A, 1600 A and 2400 A.

B. *IGBT's Gate Units*

According to the already said, there is only the need to replace the A2 and A3 units. In the replacement of these units it is important to consider two aspects: the drivers cannot be larger than the A2 and A3 units (the dimensions of these are 20cm×10cm×15cm) and must necessarily contain integrated protections against short-circuit.

Therefore, the gate units that are used for each one of the models are:

- The gate driver C0044BG400SBC to the 1200 A model;
- The gate driver C0044BG400SBJ to the 1600 A model;
- The gate driver C0044BG400SBT to the 2400 A model;

V. M1 AND M2 SNUBBERS

In this section it is discussed the operation of snubber circuits to limit, not only the values of dv_{AK}/dt and di_{GTO}/dt of the GTO's, but also the rates of switching of the freewheeling diode. The snubber used in the converter is the Undeland snubber [22].

A. *GTO Snubbers*

The circuit where the GTO drives a load with a freewheeling diode in parallel, has a snubber with capacitors, diodes, a resistor and an inductance. The snubber is formed by C_v and C_{oV}, the V5 and V6 diodes, the L_v inductance and the resistance R_{ext}.

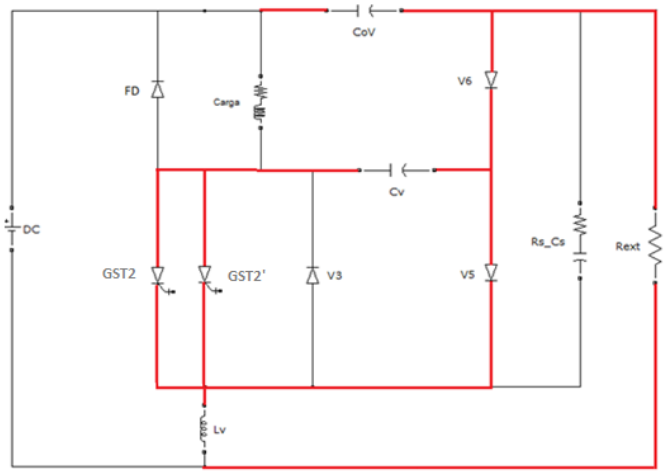

Figure 14 - GTO's snubber.

The C_v capacitor is used to ensure that the dv_{AK}/dt rate is not exceeded. In the turn-off commutation, the i_{GTO} current will flow through the freewheeling diode and C_v is given by:

$$C_v \frac{dv_{AK}}{dt} = i_{GTO} \tag{15}$$

With $dv_{AK}/dt = 500/1 \times 10^{-6}$, $C_{vmin} \approx 1{,}56\ \mu F$.

The L_v inductance is used to limit the di_{GTO}/dt rate and is determined by:

$$L_v \frac{di_{GTO}}{dt} = U \tag{16}$$

With $di_{GTO}/dt = 200/(1 \times 10^{-6})$, we obtain $L_v \approx 3{,}75\ \mu H$. This inductance has also the purpose of limit the maximum reverse current of the freewheeling diode.

The snubber resistance R_{ext}, is determined to almost dampen the current that flows through the GTO during the turn-on commutation and the GTO's minimum period in which the C_v is discharged. Therefore,

$$R_{ext} \approx 2\xi \sqrt{L_v / C_v} \tag{17}$$

With $\xi = 0{,}8$, results $R_{ext} \approx 2{,}48\ \Omega$.

The C_{OV} capacitor has the goal of protecting the overvoltages from the parasitic inductances, acting simultaneously with C_v and R_{ext}. This capacitor can be determined using:

$$\frac{1}{2}C_v V_{DC}^2 \rightarrow \frac{1}{2}C_{OV}\Delta V_{DC}^2 \qquad (18)$$

Therefore, supposing $\Delta V_{DC}^2 = V_{DC}^2/10$, we obtain $C_{OV} = 15{,}6\ \mu F$.

B. *GTO's turn-on and turn-off commutations*

In figures 16 and 17 it is illustrated the waveforms of the GTO's at the turn-on and turn-off commutation, under the influence of the snubber previously determined.

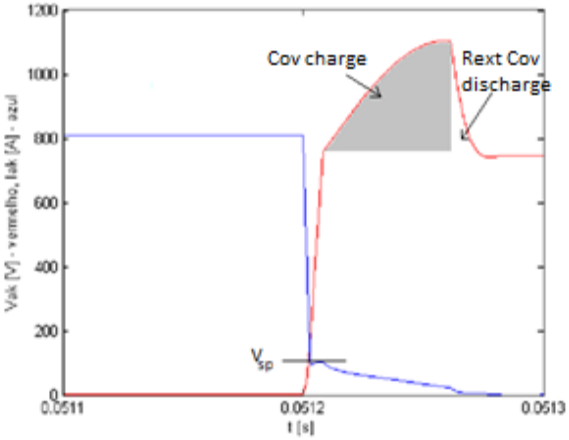

Figure 15 - GTO's turn-off commutation.

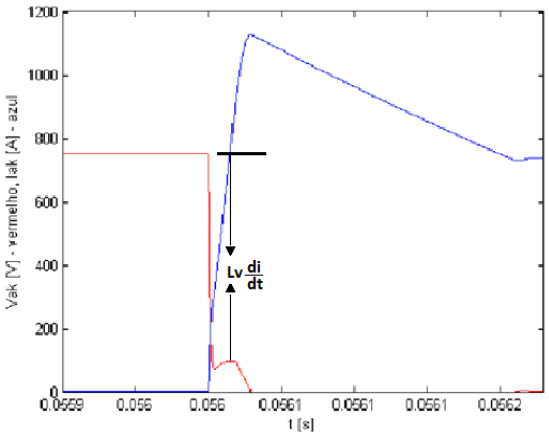

Figure 16 - GTO's turn-on commutation.

C. *Freewheeling diode snubber*

In figure 17 it's underlined the diodes snubber current path. The diodes snubber is constituted from the R_sC_s series and the L_v inductance.

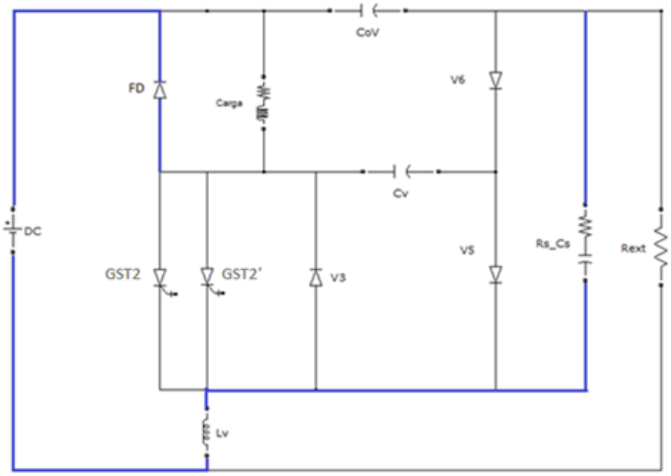

Figure 17 - Freewheeling diode snubber.

The C_s capacitor is given by [1]:

$$C_s = 1{,}5\frac{Q_{RR}}{U} \qquad (19)$$

With $Q_{RR} = 400\ \mu As$, we obtain $C_s \approx 0{,}8\ \mu F$.

On the other hand, R_s is determined according to equation (17), using $\xi \approx 0{,}65$, results $R_s \approx 2{,}81\ \Omega$.

D. *Determination of the M1/M2 efficiency*

The total efficiency of each module is determined according to:

$$\eta = \frac{P_0}{P_0 + P_{losses}} \qquad (20)$$

With,

$$P_{losses} = P_{díodes} + P_{GTO's} + P_{snubbers} \qquad (21)$$

$$P_{GTO's} = 2\left(P_{d_{GTO}} + P_{S_{GTO}} + P_{S_{OFFGTO}}\right) \qquad (22)$$

$$P_{díodes} = P_{d_{díode}} + \left(3\,P_{S_{OFFdíode}}\right) \qquad (23)$$

$$P_{d_{díodo}} = V_D\,I_{FDC} + r_D I_{FRMS}^2 \qquad (24)$$

$$P_{S_{OFFdíodo}} = \frac{V_{RR} I_{RR}}{T}(t_{RR} - t_s) \qquad (25)$$

$$P_{snubberGTO} = \frac{1}{2}\,C_V\,U^2\,f \qquad (26)$$

$$P_{snubberdíodo} = \left[\frac{1}{2}\,C_s\,U^2 + \frac{1}{2}\,L_v\,{I_{RR}}^2\right] f \qquad (27)$$

Considering that V5 and V6 have only commutation losses, due to their short conduction period, we obtain $P_{losses} \approx 3027{,}40$ W.

So,

$$\eta = \frac{468\times10^3}{468\times10^3 + 2767{,}75} \approx 0{,}9941 = 99{,}41\% \qquad (28)$$

The efficiency of each one of the modules is very high, since the GTO's switching frequency is very low.

E. Heatsink determination

In the converter module studied, a direct air-cooled unit is used to cool the semiconductors.

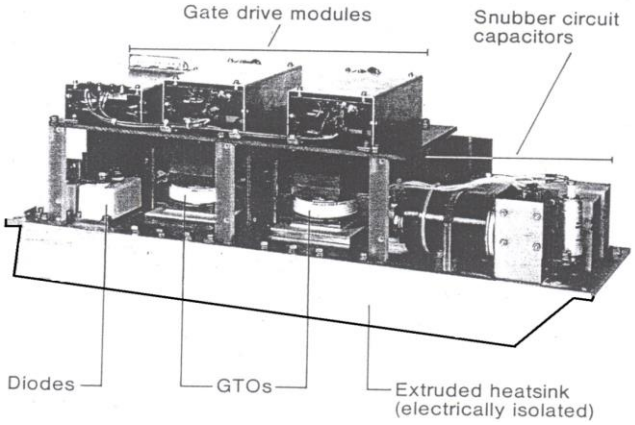

Figure 18 - Converter module with GTO's and direct air cooling.

To understand the kind of used heatsink, we need to determine the respective thermal resistance between the sink and the environment (R_{ths-a}). The equivalent thermal resistances model of the M1 Module is illustrated in figure 19.

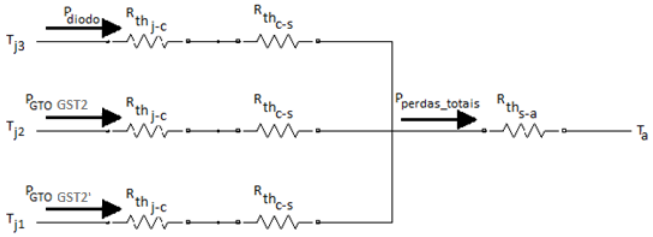

Figure 19 - Equivalent thermal resistances model of the M1 Module.

Therefore, R_{ths-a} is given by:

$$R_{ths-a} = \frac{(T_{jmax}-T_a)-(R_{thj-c}+R_{thc-s})P_{GTO}}{P_{perdas\_totais}} \quad (29)$$

Obtaining, $R_{ths-a} \approx 0{,}0227\ ℃/W$.

VI. Replacing the GTO's by IGBT's

When replacing the GTO' by the Press-Pack IGBT's there are two approaches to be studied: first a direct replacement, where only the GTO's and their gate units are replaced; second, a replacement where some optimization is made in the snubber circuit.

A. Like for like replacement

In this replacement strategy only the GTO's (and their gate units) are replaced by the Press-Pack IGBT's (and respective gate units), remaining intact all the other components of the modules. Considering that,

$$P_{losses} = P_{diodes} + P_{IGBT's} + P_{snubbers} \quad (30)$$

With,

$$P_{IGBT's} = 2\left(P_{d_{IGBT}} + P_{S_{IGBT}}\right) \quad (31)$$

$$P_{dIGBT's} = V_{CEsat}\, i_{c_{DC}} + r_{CE} I^2_{c_{RMS}} \quad (32)$$

$$P_s = V_{CC}\ I_{CC} \frac{(a^2\, t_{fGTO} + b^2\, t_{rGTO})}{6T} \quad (33)$$

With $t_{fIGBT} = a\, t_{fGTO} (a<1)$ and $t_{rIGBT} = b\, t_{rGTO}$ $(b<1)$ results for the three Press-Pack IGBT's models:

IGBT	P_{losses}[W]	η [%]
T1200EB45E	2220,09	99,55
T1600GB45G	2209,33	99,56
T2400GB45E	1928,31	99,61

Table 1 - M1 efficiency with the three kinds of IGBT's.

These strategy does not take advantages that IGBT's offer over GTO's, because the M1/M2 modules works under low switching frequency (250 Hz). To higher rates of commutation, the difference between the IGBT switching losses and the GTO switching losses would be more striking. Besides, we verify that the efficiency of the M1/M2 Modules are higher for the 3 IGBT's considered.

B. Replacement with optimization

The optimization consists in reducing the snubber capacitance accordingly to the intrinsic capability that IGBT's have in supporting much higher dv/dt rates than the GTO's.

Therefore, it is economically viable to reduce the C_v capacitor to half of his value, this is, $C'_v = C_v/2 = 0{,}78\ \mu F$.

With this strategy, the snubber losses are reduced by 50%, and we obtain:

IGBT	P_{losses}[W]	η [%]
T1200EB45E	2065,24	99,56
T1600GB45G	2010,60	99,57
T2400GB45E	1747,76	99,63

Table 2 - M1 efficiency with C_v reduced to half.

The results confirm that the optimization leads to a slight improvement in overall efficiency, without having adverse effects.

VII. SIMULATIONS

A. GTO switching

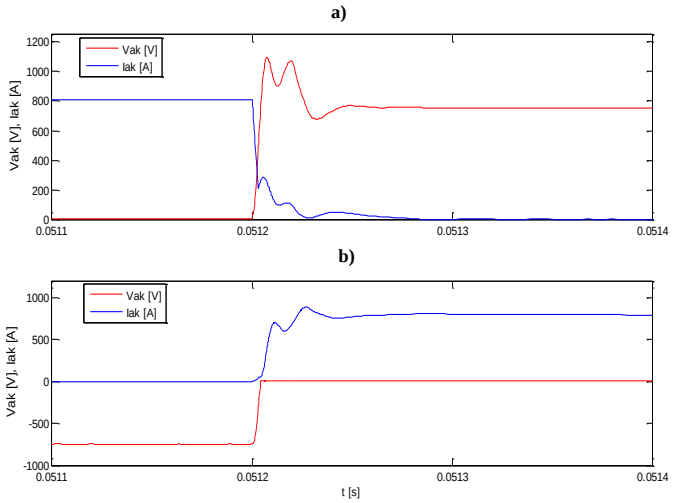

Figure 20 - a) GTO's turn-off commutation; b) Freewheeling diode's turn-on commutation.

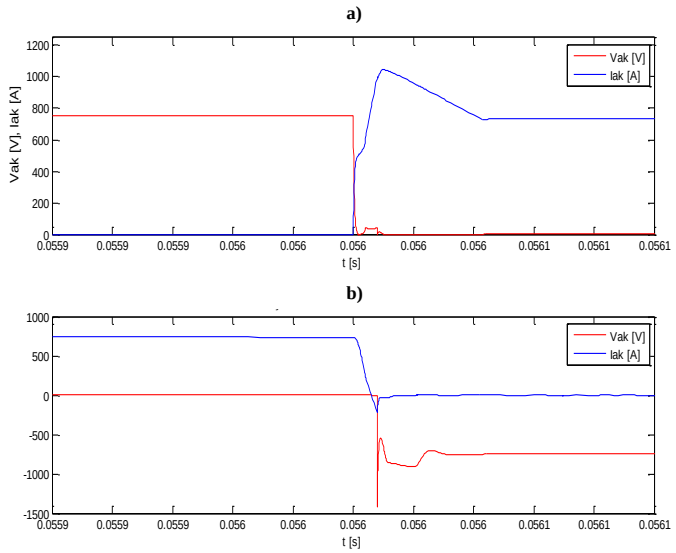

Figure 21 - a) GTO's turn-on commutation; b) Freewheeling diode's turn-off commutation.

The efficiency obtained to the M1 Module, with the *Matlab/Simulink* program was 99,22%. This result is similar (less than 0,20% error) to the one obtained in the theoretical study (99,41%), revealing that the used theoretical models are valuable tools to do prior estimations.

B. IGBT's switching

In this paper we only present the waveforms for the 2400 A IGBT. The waveforms for the other two models also demonstrate that the *Matlab/Simulink* model confirms what was obtained in the theoretical study.

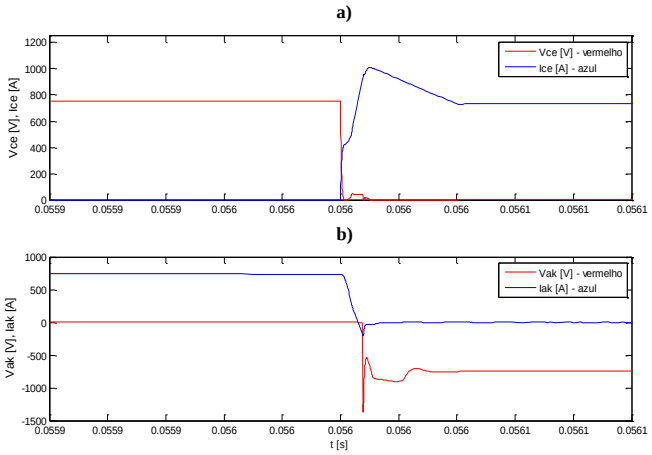

Figure 22 - a) IGBT's turn-on commutation; b) Freewheeling diode's turn-off commutation.

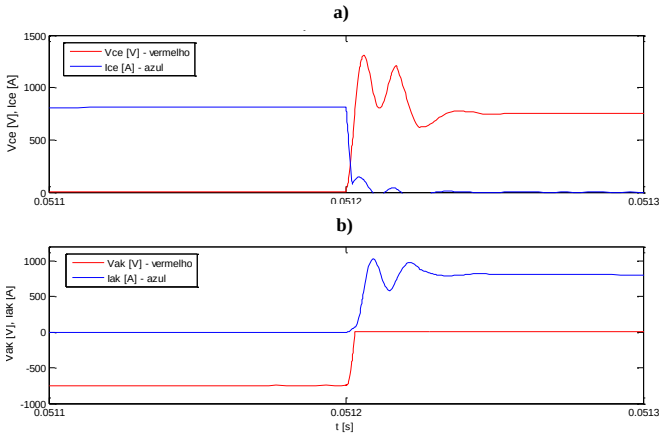

Figure 23 – a) IGBT's turn-off commutation; b) Freewheeling diode's turn-on commutation.

Being the efficiency (≈ 99,44%) similar to 99,61% (Table 1).

With $C_v = C_v/2$, the waveforms are:

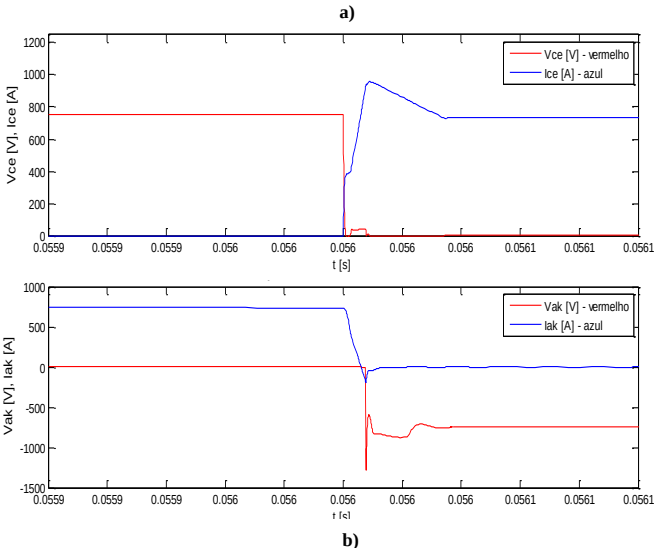

Figure 24 - a) IGBT's turn-on commutation; b) Freewheeling diode's turn-off commutation.

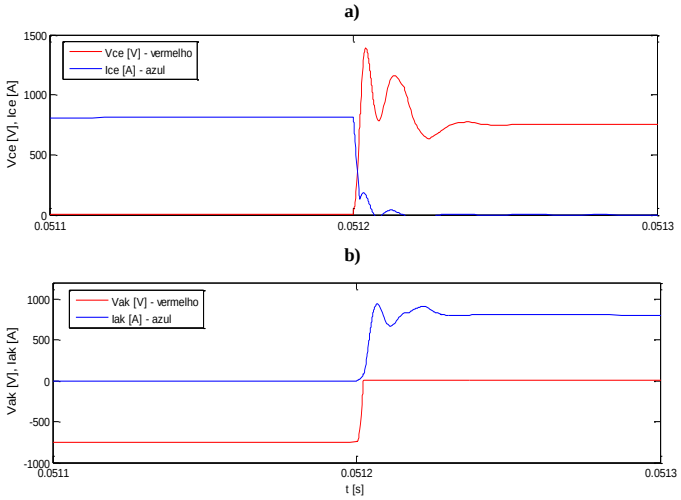

Figure 25 – a) IGBT's turn-off commutation; b) Freewheeling diode's turn-on commutation.

With $\eta = 99{,}45\%$, closed to the theoretical value 99,63% (Table 2).

Comparing figures 23 and 25, we can conclude that reducing the C_v capacitor to half of his value, aggravates a little the v_{AK} overvoltage in the IGBT's turn-off commutation. However, this slight change is not significant, due to IGBT's intrinsic capability in supporting much higher dv/dt rates than the GTO's. This proves that the C_v capacitor value reduction is a viable option, since there is less power to be dissipated in the IGBT's commutations without jeopardizing their operation.

Analyzing figures 22 and 24, we also observe that the modification in the snubber circuit has positive effects in IGBT's turn-on commutations, being the i_{AK} overcurrent less marked to the lowest value of C_v.

On the other hand, the above figures shows that the overvoltages and peak current obtained for the GTO's and IGBT's simulation are supportable by the devices, according to the manufacturers specifications.

VIII. Conclusions

During this work, we have verified – through theoretical studies and simulations via *Matlab/Simulink* – that the replacement of GTO thyristors in the M1 and M2 Modules by Press-Pack IGBT's (manufactured by *Westcode*) is a viable option to solve the GTO's obsolescence.

The results, both theoretically and in simulation, show that any of the 3 IGBT's models leads to less losses than the GTO's, so that the overall efficiency of the converter is always higher using this type of device. It was also proved that the 2400 A IGBT offers the best results (less losses and higher efficiencies) for the two replacement strategies.

It was observed that reducing the C_v capacitor to half of his value, when using IGBT's, slightly improves the M1 and M2 Modules efficiency (compared to the direct replacement strategy) due to IGBT's intrinsic potential in supporting higher dv/dt rates.

It was also noted that the drivers of the three Press-Pack IGBT's are suitable (in dimensions and specifications) to replace the GTO's drivers.

As future work, it would be interesting to experimentally validate the proposed solution, making the replacement of GTO's and its gate units for Press-Pack IGBT's and its gate units.

References

[1] J. Fernando Silva, Electrónica Industrial: Semicondutores e Conversores de Potência, série Manuais Universitários, Fundação Calouste Gulbenkian, Lisboa, ISBN 978-972-31-1499-7, 740 pp, 2013.

[2] Paixão, Bruno da Silva Campos; "Conversor de tracção do material circulante ML90 do Metropolitano de Lisboa", Instituto Superior Técnico, Junho 2010.

[3] Rahimo, M.T. e Shammas, N.Y.A; "Freewheeling Diode Reverse Recovery Failure Modes in IGBT Applications", Institute of Electrical and Electronics Engineers, March/April 2001.

[4] Mendes, Katila Sofia de Freitas; "Ensaio do comando do conversor de tracção do material circulante ML90 do Metropolitano de Lisboa", Instituto Superior Técnico, Outubro 2010.

[5] Haaf, Peter e Harper, Jon; "Understanding Diode Reverse Recovery and its Effect on Switching Losses", Fairchild Semiconductor Europe, 2007.

[6] R. Alvarez, F. Filsecker e S. Bernet; "Comparison of Press-pack IGBT at Hard Switching and Clamp Operation for Medium Voltage Converters", Power Electronics and Applications (EPE 2011), Proceedings of the 2011-14th European Conference on, Aug.30 2011 – Sept.1 2011

[7] A. Golland e F. Wakeman; "Third Generation Press-pack IGBT's and Diodes for Megawatt Applications", Westcode Semiconductors Ltd, Chippenham, UK.

[8] A. Golland , F. Wakeman e G.Li; "New family of 4.5kV Press-pack IGBT's", Westcode Semiconductors Ltd, Chippenham, UK, Junho 2005.

[9] A. Golland , F. Wakeman e G.Li; "Managing power semiconductor obsolescence by press-pack IGBT substitution", Westcode Semiconductors Ltd, Chippenham, UK, 2005.

[10] A. Golland , F. Wakeman; "Application of Press-pack IGBT's in Traction Refurbishment", Westcode Semiconductors Ltd, Chippenham, UK, February 2005.

[11] F. Wakeman, W. Findlay e G. Li; "Press-pack IGBT's, semiconductor switches for pulse power", Westcode Semiconductors Ltd, Chippenham, UK.

[12] F. Wakeman, D. Hemmings, W. Findlay e G.Lockwood; "Pressure contact IGBT, testing for reliability", Westcode Semiconductors Ltd, Chippenham, UK.

[13] F. Wakeman, K. Billett, R. Irons e M. Evans; "Electromechanical characteristics of a bondless pressure contact IGBT", Westcode Semiconductors Ltd, Chippenham, UK.

[14] M.J. Evans, F.J. Wakeman, R.I. Irons, G.W. Lockwood e K.R. Billet; "Design concepts of a bondless pressure contact IGBT", Westcode Semiconductors Ltd, Chippenham, UK.

[15] F. Wakeman, G.Lockwood e M. Davies; “New high reliability bondless pressure contact IGBT’s”, Westcode Semiconductors Ltd., 2002.

[16] Bernet, Steffen; “Function, Technology and Features of IGCTs and High Voltage IGBT’s”, Berlin University of Technology, Berlin, Germany, Setembro 2003.

[17] N. D. Benavides, T. J. McCoy e M. A. Chrin; “Reliability Improvements in Integrated Power Systems with Pressure-Contact Semiconductors”, Converteam Naval Systems Inc., Pittsburgh.

[18] E. R. Motto e M. Yamamoto; “New High Power Semiconductors: High Voltage IGBT’s and GCTs”, Powerex Inc., Youngwood, Pennsylvania, USA e Mitsubishi Electric, Power Device Division, Fukuoka, Japan

[19] M. F. Furuya e Y. Ishiyama; “Current Measurement Inside Press Pack IGBT’s”, Fuji Electric Journal, Vol.75 No.8, 2002.

[20] R. Alvarez, F. Filsecker e S. Bernet; “Comparison of Press-pack IGBT at Hard Switching and Clamp Operation for Medium Voltage Converters”, Power Electronics and Applications (EPE 2011), Proceedings of the 2011-14th European Conference on, Aug. 30 2011-Sept. 1 2011.

[21] A. Müsing, G. Ortiz, e J. W. Kolar; “Optimization of the Current Electronics Conference.

[22] N. Mohan, T.M. Undeland e W.P. Robbins; “Power Electronics: Converters, Applications and Design”, 2nd Editions.

[23] Silva, J F; Santana, J; Pinto, S F; “Conversores Comutados para Energias Renováveis”, Texto de apoio, IST, 2013. Distribution in Press-pack High Power IGBT Modules”, The 2010 International Power

[24] Miguel Chaves, Elmano Margato, S. Pinto, J. Fernando Silva, New Approach in Back-to-Back m Level Diode-Clamped Multilevel Converter Modeling and DC Bus Voltages Balancing, IET Power Electronics, Volume: 3 Issue:4, pp578 – 589, 2010, July, ISSN: 1755-4535.